In situ characterization of preferential flow by combining plot- and point-scale infiltration experiments on a hillslope

In situ characterization of preferential flow by combining plot- and point-scale infiltration experiments on a hillslope

Article *in* Journal of Hydrology · June 2018

DOI: 10.1016/j.jhydrol.2018.06.033

CITATIONS
15

READS
276

5 authors, including:

Simone Di Prima
Università degli Studi di Sassari
96 PUBLICATIONS **1,059** CITATIONS
SEE PROFILE

Roberto Marrosu
Università degli Studi di Sassari
16 PUBLICATIONS **56** CITATIONS
SEE PROFILE

Laurent Lassabatere
Ecole Nationale des Travaux Publics de l'Etat
189 PUBLICATIONS **1,804** CITATIONS
SEE PROFILE

Mario Pirastru
Università degli Studi di Sassari
44 PUBLICATIONS **407** CITATIONS
SEE PROFILE

In situ characterization of preferential flow by combining plot- and point-scale infiltration experiments on a hillslope

S. Di Prima[1,*], R. Marrosu[1], L. Lassabatere[2], R. Angulo-Jaramillo[2], M. Pirastru[1]

[1] Agricultural Department, University of Sassari, Viale Italia, 39, 07100 Sassari, Italy
[2] Université de Lyon; UMR5023 Ecologie des Hydrosystèmes Naturels et Anthropisés, CNRS, ENTPE, Université Lyon 1, 3 rue Maurice Audin, 69518 Vaulx-en-Velin, France
[*] Corresponding Author: E-mail: sdiprima@uniss.it

This is a post-refereeing final draft. When citing, please refer to the published version:

Di Prima, S., Marrosu, R., Lassabatere, L., Angulo-Jaramillo, R., Pirastru, M., 2018. In situ characterization of preferential flow by combining plot- and point-scale infiltration experiments on a hillslope. Journal of Hydrology 563, 633–642. https://doi.org/10.1016/j.jhydrol.2018.06.033

Abstract

This study focuses on the identification of the lateral preferential flow at the hillslope scale and the estimation of the saturated hydraulic conductivity for the fast-flow region, $K_{s,f}$, based on infiltration experiments carried out at different spatial scales (point- and plot-scales), and at different soil depths. The discrepancies between the considered scales were mainly attributed to macropore flow and the difficulty in adequately embodying the macropore network on small sampled soil volumes. Conversely, at the plot-scale, the sampled volume was sufficient to activate the macropore network. This information helped establish the usability of a given technique to determine the parameters describing the hydraulic properties of the soil in the matrix and fast-flow regions. While K_s data obtained from the Beerkan method with the Beerkan Estimation of soil Transfer (BEST) parameter algorithm (point-scale) were used to describe the matrix ($K_{s,m}$), the saturated hydraulic conductivity for the fast-flow region was estimated using the soil block method (plot-scale). Estimated $K_{s,f}$ values were one to three orders of magnitude higher than $K_{s,m}$. The overall decrease of $K_{s,f}$ with the soil depth supported the hypothesis that the macropore density decreased as a function of depth, yielding higher macropore flow variability. The soil block method, in association with the Beerkan infiltration runs, allowed the estimation of the saturated hydraulic conductivity for the fast-flow region based on a relatively simple field procedure.

Keywords: Beerkan, BEST algorithm, in situ soil block method, cube method, lateral preferential flow, macropore.

1. Introduction

Scarcity of water has been universally recognized as a global issue (Vörösmarty et al., 2000). Climatic changes have profound effects on the hydrological cycle, thus reducing the availability of water resources in many environments (Groppelli et al., 2011). In semiarid and arid regions, increasing demands on limited water supplies require urgent efforts to improve water quality and quantity by preserving and improving the groundwater recharge of surface water bodies (Scanlon et al., 2006). Recharge processes can be classified as uniform downward movements of water through the unsaturated zone (piston flow), and nonuniform downward water movement along more active pathways, also referred to as preferential flow (Sukhija et al., 2003). Preferential flow can contribute to the rapid transport of contaminants from the soil surface into receiving streams, bypassing the filtering capacity of the soil (e.g., Lamy et al., 2009; Lassabatere et al., 2007; Prédélus et al., 2017). Water flow may mainly occur via preferential flow paths (Blöschl and Sivapalan, 1995), especially at the hillslope scale. Therefore, there is an urgent need to assess procedures and techniques for characterizing water transport in hillslopes especially when this transport appears to be affected by preferential flow paths, which may be induced by structural cracks, faunal activity or roots, specific pedological conditions, and soil management practices (Angulo-Jaramillo et al., 2016).

The saturated soil hydraulic conductivity, K_s, exerts a dominating influence on the partitioning of rainfall in vertical and lateral flow paths (Dusek et al., 2012). Therefore, estimates of K_s are essential for describing and modeling hydrological processes (Niedda and Pirastru, 2013; Zimmermann et al., 2013). However, this soil property may be scale-dependent mainly owing to the soil structure, preferential flow paths, and heterogeneities, whose effects cannot be observed and quantified in measurements conducted on small soil volumes. In addition, the scale dependence of flow and transport parameters essentially makes the use of parameters estimated through pedotransfer functions for numerical simulations impossible (Pachepsky et al., 2014). The saturated hydraulic conductivity must be measured in the laboratory or field. Several studies have shown that the saturated soil hydraulic conductivity values, K_s, measured on macroporous soils, can vary over several orders of magnitude depending on the sampled soil volume (Chapuis et al., 2005). For instance, Vepraskas and Williams (1995) compared K_s values using

sample volumes equal to 3.5×10^{-4}, 6.3×10^{-3}, and 6.8×10^{-1} m^3, concluding that the minimum sample size needed in situ for K_s measurements ought to be approximately equal to at least 5×10^{-3} m^3. Experiments used to determine K_s values at different spatial scales were performed by Chappell and Lancaster (2007). These authors applied six field methods, namely slug tests, constant- and falling-head borehole permeameters, a ring permeameter and two types of trench tests. The K_s values determined by the larger scale experiments, i.e., the trench percolation tests were, on average, 37 times larger than the mean conductivity obtained by slug tests conducted using piezometers positioned near the trenches (Chappell and Lancaster, 2007). Brooks et al. (2004) discussed different reasons to explicate such a discrepancy. For instance, small samples may not adequately represent water transmission, since smaller sampled volumes imply a smaller opportunity to include macropores (Zobeck et al., 1985). In particular, the extent of the macropores in the porous medium was considered as the main factor in determining the gap between measurements.

Hillslope-scale measurements overcome the lack of representativeness commonly encountered in small-scale measurements and allow process characterization at the appropriate scale. These types of measurements are therefore recommended for model calibration. However, the number of studies that have focused on the assessment of large-scale experiments and their comparisons with smaller-scale experiments have been limited. Among the studies that focused on large-scale experiments, those that have addressed preferential or macropore flows are particularly few. Montgomery and Dietrich (1995) compared the hydraulic conductivity calculated from a gully head cut with those observed in falling head tests. Only the higher values obtained from this latter experiment approached the bulk conductivity measured from the gully head cut by integrating through- and macropore flows. Brooks et al. (2004) proposed a methodology to measure the lateral K_s values at the top of an impeding layer at the hillslope scale. Their measurements yielded K_s values from one to two orders of magnitude larger than those measured at small-scales on small soil cores and by using the Guelph permeameter. The discrepancy between measurements at different spatial scales was greatest near the surface and was attributed to the effect of the macropores. Furthermore, according to these authors, more economical methods are needed to obtain spatially distributed K_s data, or for routine measurements (Brooks et al., 2004). Reliable K_s values should be measured on a soil volume similar to the minimum representative elementary volume (REV) to incorporate the natural heterogeneity of the soil (Mendoza and Steenhuis, 2002). The REV is the smallest volume over which a measurement can be made to yield a representative value of the entire porous medium (Pachepsky and Hill, 2017). Its size depends on the soil structural characteristics and it is expected to increase for decreasing macropore spatial densities. Thus, in order to adequately represent the hydrological effects of the macropore network, the REV should include a sufficient number of nodes and branches in such a way to representatively embody the macropore network topology since it may control scale dependencies.

The in situ block method (Day et al., 1998) has proven to be a useful tool for saturated soil hydraulic conductivity measurements. This technique consists of measuring water flow in situ on a large, undisturbed soil block that seals the exposed sides in order to confine water flow. For example, Day et al. (1998) measured water flow on a 3.38 m^3 soil block. The block's vertical faces were sealed using bentonite, sand, and lumber. Blanco–Canqui et al. (2002) evaluated K_s on three, in situ, 0.029 m^3 soil blocks enclosed by steel plates, and inserted approximately 35 cm below the soil surface and on bentonite-slurry to seal the soil–steel plate interfaces. Mendoza and Steenhuis (2002) developed and tested a hillslope infiltrometer to measure in situ vertical and lateral saturated soil hydraulic conductivity. The hillslope infiltrometer is a metal box installed around an undisturbed 0.045 m^3 soil block slightly smaller than the infiltrometer. Starr et al. (2005) designed an in situ steel chamber for studying water flow under shallow water table and riparian zone conditions. The chamber was lowered over a 0.97 m^3 soil block. However, K_s measurements on the soil block remain rare for the following reasons: i) the need for a sloping impermeable bed to avoid deep-water percolation, ii) the need to encase a large soil volume with impermeable materials so that all terms of Darcy's law can be unambiguously defined, iii) the need for a number of operators over the entire duration of the experiment, and the iv) the need of a large displacement of liquid to reach steady state conditions during flow measurements.

Several studies have considered small-scale measurements on macroporous soils including both laboratory and in situ tests (Akay et al., 2008). These approaches are generally simpler and parsimonious in terms of the experimental devices and required measurements. However, small-scale measurements may not adequately represent K_s depending on whether water flows through a small fraction of the soil along preferential flow paths (Bouma et al., 1977) or only through the matrix. In fact, at this scale, macropores are hardly intercepted, while their continuity at the larger scale is unknown (Beven and Germann, 1982; Zobeck et al., 1985). Moreover, the presence of aggregates, stones, fissures, fractures, tension cracks, and root holes, commonly encountered in unsaturated soil profiles, is difficult to represent in small samples (Haverkamp et al., 1999). The dual permeability approach has been developed for modeling and for quantifying preferential flow (Gerke et al., 2015; Šimůnek et al., 2003). The dual-permeability approach assumes that soils encompass two regions, including the matrix and the fast-flow regions that respectively host the smallest and the larger pores. Lassabatere et al. (2014b) used the dual-permeability approach to model water infiltration below ponded and tension infiltrometers in heterogeneous soils. At the hillslope scale, Dusek et al. (2012) studied the preferential flow effects on the subsurface runoff by combining a one-

Di Prima, S., Marrosu, R., Lassabatere, L., Angulo-Jaramillo, R., Pirastru, M., 2018. In situ characterization of preferential flow by combining plot- and point-scale infiltration experiments on a hillslope. Journal of Hydrology 563, 633–642. https://doi.org/10.1016/j.jhydrol.2018.06.033

dimensional (1D) vertical dual-continuum approach with a 1D lateral flow equation. More recently, different innovative approaches were proposed for dual- and multiple-permeability medium characterizations. For instance, Abou Najm and Atallah (2016) proposed a new method to experimentally characterize porous media by using Newtonian and non-Newtonian fluids. Lassabatere et al. (2014a) proposed the BEST–2K method for hydraulic characterization of dual permeability media on the infiltration data acquired on the field. However, all these methods need to be further developed and tested to address processes at the small scale (i.e., maximum meter scale).

The objective of this research was to characterize and quantify a lateral preferential flow at the hillslope scale. For this purpose, we considered the double permeability approach (concomitancy of fast-flow and matrix regions) and estimated the saturated hydraulic conductivities of both fast-flow and matrix regions, $K_{s,f}$ and $K_{s,m}$, by coupling data from the infiltration experiments carried out at different spatial scales, namely, at point- and plot-scales. Specifically, we combined the following experiments: (i) in situ, small scale measures of soil vertical hydraulic conductivity using the Beerkan method, (ii) laboratory small scale measures of vertical and horizontal hydraulic conductivity using the modified cube method, and (iii) plot-scale measure of lateral hydraulic conductivity using in situ soil blocks. We assumed that Beerkan runs would help the determination of the saturated hydraulic conductivity of the matrix and the modified cube method in the determination of the vertical and horizontal hydraulic conductivity of the soil. These measures are then used to analyze the observed flow through the soil blocks and to identify and quantify the contribution of the matrix and the macropore network to the total lateral flux as a function of the volume of the soil block that is submitted to lateral flow.

2. Material and methods

2.1. Study site description

The study area consists of a north-facing steep slope side located in the Baratz Lake basin (Niedda et al., 2014) on Sardinia's North–West coast in Italy (40.69825 N, 8.2346 E, WGS84). The site features a semiarid Mediterranean climate with a mild winter, warm summer, and a high water deficit between April and September. The mean annual temperature is 15.8°C. The average annual precipitation is approximately 600 mm, mainly concentrated from autumn to spring. The potential evapotranspiration is approximately 1000 mm year^{-1}. The experimental hillslope has elevations ranging from 51 to 65 m a.s.l., and it is approximately 60 m long, and with an average slope of 30%. While the incoming surface and subsurface flows are diverted by the ditches on both sides of a road at the upper end, the hillslope is drained by the main stream channel of the catchment at the toe. The hillslope soil was classified as a Lithic Haploxerepts (Soil Survey Staff, 2006). Its profile is approximately 0.3–0.4 m deep. The soil horizons include A, Bw, and C (Pirastru et al., 2014). The latter is a dense altered substratum of Permian sandstone which exhibits very low permeability (Castellini et al., 2016). During the rainy season, a perched water table and lateral subsurface flow were observed owing to the presence of this restrictive layer. In terms of vegetation, the experimental area is covered with spontaneous grass grown after the clearing of the Mediterranean maquis and deep moldboard ploughing. The conversion into grassland took place approximately 15 years ago in order to create a 15 m wide firebreak. The area has remained almost unmanaged ever since.

2.2. Soil sampling

Soil samples were collected at depths of 0, 5, 10, 20 cm. In particular, undisturbed soil cores (0.05 m in height and 0.05 m in diameter) were collected at randomly sampled points and were used to determine both the soil bulk density, ρ_b (g cm^{-3}), and the initial volumetric soil water content, θ_i (cm^{3}cm^{-3}). The soil porosity was calculated from the ρ_b data, assuming a soil particle density of 2.65 g cm^{-3}. According to other investigations, the field's saturated soil water content, θ_s (cm^{3}cm^{-3}), was equal to the porosity (Di Prima et al., in press; Mubarak et al., 2009).

Disturbed soil samples were also collected inside the confined soil after each ponding infiltration runs and was used (50 g for each sample) to determine the particle size distribution based on conventional methods following H_2O_2 pretreatment to eliminate organic matter and clay deflocculation using sodium metaphosphate and mechanical agitation (Gee and Bauder, 1986). In particular, fine size fractions were determined using the hydrometer method, whereas the coarse fractions were obtained by mechanical dry sieving. According to USDA standards, the soil of the studied area was classified as sandy loam. According to Shirazi and Boersma (1984), the geometric mean particle diameter was also estimated. **Table 1** summarizes the physical parameters of the soil at the studied hillslope.

2.3. In-situ block method

The soil block method aimed at including the lateral component of the preferential flow at the plot scale for lateral K_s measurements. More details on the soil block preparation can be found in Di Prima et al. (2017b) and Pirastru et al. (2017). At first, four soil blocks with dimensions of 50 cm (width) by 105 cm (length) by 70 cm (depth) were obtained by careful hand digging of trenches with widths of 20 cm surrounding each soil block. Since the interface between the upper horizons and the restrictive substratum was located at a depth of approximately 38 cm, the excavated soil blocks consisted of layered blocks, and included the upper A and Bw horizons, and approximately 32 cm of impeding substratum. No evidence of man-made cracks was observed during the excavation process. Expandable polyurethane foam was then

Di Prima, S., Marrosu, R., Lassabatere, L., Angulo-Jaramillo, R., Pirastru, M., 2018. In situ characterization of preferential flow by combining plot- and point-scale infiltration experiments on a hillslope. Journal of Hydrology 563, 633–642. https://doi.org/10.1016/j.jhydrol.2018.06.033

Table 1. Clay (%), silt (%) and sand (%) content (U.S. Department of Agriculture classification), geometric mean particle diameter, d_g (mm), dry soil bulk density, ρ_b (g cm^{-3}), initial soil water content, θ_i (cm^3 cm^{-3}), and saturated soil water content, θ_s (cm^3 cm^{-3}), for the four sampled soil depths. The coefficients of variation (%) are listed in parentheses.

Soil depth (cm)	0	5	10	20
Sample size	10	10	10	9
Clay	17.4 (28.6)	19.5 (18.6)	20.2 (25.1)	23.2 (20.7)
Silt	28.8 (8.9)	29.2 (10.2)	28.3 (7.7)	27.9 (9.2)
Sand	53.8 (12.6)	51.4 (9.8)	51.5 (13.3)	48.9 (14.4)
d_g	0.114 (37.1)	0.095 (30.7)	0.096 (37.3)	0.080 (43.7)
Sample size	3	3	3	3
ρ_b	1.56 (3.0)	1.66 (7.1)	1.55 (6.2)	1.52 (3.0)
θ_i	0.23 (18.3)	0.25 (4.1)	0.18 (15.0)	0.18 (10.3)
θ_s	0.41 (4.3)	0.37 (11.9)	0.42 (8.7)	0.43 (4.0)

injected into the trench volumes in order to encase the exposed soil blocks. This inert material is not expected to alter the chemical (Lewis et al., 1990) and physical (Bagarello and Sgroi, 2008) characteristics of the soil, and it concurrently prevents edge flows (Germer and Braun, 2015). After the foam was completely dried, two pits were excavated up to the depth of the soil–substratum interface in order to expose the up- and downhill faces of the soil block and to create inflow (IP) and outflow pits (OP), respectively. At the end, the resulting soil blocks, hereafter referred to as SBs, were associated with a geometrically calculated volume above the impeding layer that ranged from 0.100 to 0.163 m^3. Each drainage experiment consisted of four stages. After a first satiation stage, three water table depths (WTDs, **Figure 1**) were sequentially settled at 5, 15, and 25 cm below the soil surface in the IP with a custom-built Mariotte bottle. The large 50 L capacity of the bottle avoided the need of frequent refilling throughout the duration of the executed stages. Each imposed water table depth was maintained until the achievement of quasi-steady-state conditions. A syphon system was used to impose from time to time the same water table depths in the OP. During these processing stages, visual readings of the water level in the bottle were used to calculate the inflow rates, as obtained through a liquid-level gauge. The excess water flowing from the OP through the syphon system was measured by weighting the collected water volumes. **Figure 2** depicts the experimental setup. The total run duration varied between 260 and 460 min, depending on the run.

A first attempt to measure outflow from the OP was carried out using a 4 cm diameter PVC pipe used as a spillway. At the downhill side, the pipes were inserted in the dried foam at a smooth slope in order to maintain a constant water level and to divert the excess volume for collection. This procedure was applied only on the SB1 because field observations revealed that the pipe installations produced a slight discontinuity between soil and foam, thus resulting in leakages. To avoid

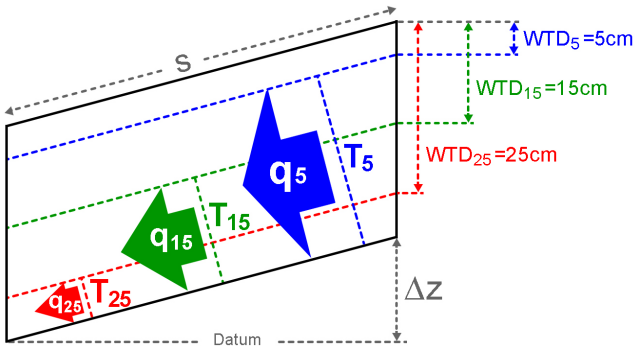

Figure 1. Schematic diagram of a drainage experiment carried out on a soil block. Measured flows per unit width of the block (q_{WTD}) and thickness of the flow zones (T_{WTD}) for different water table depths (WTDs), distances along the sloping bed (s), and water table elevation from an arbitrary datum (ΔZ).

such a problem, the syphon system was used for the other soil blocks (**Figure 2**). Therefore, for these latter experiments, the water loss was small, thus yielding similar inflow and outflow measurements (**Figure 3**). However, in the third and fourth SBs, the same differences between inflow and outflow rates were detected for WTD_{25}. In particular, water draining from progressive desaturation of the upper soil volume (i.e., the layer that had a depth that ranged between 15 and 25 cm) initially contributed to yield higher outflows. During this stage, the desaturation of the upper soil volume did not affect the inflow rates since the flow zone was already saturated during the previous stages of the experiment. This difference was not observed in the SB2 experiment probably owing to the higher measured flow rates (**Figure 3**). Therefore, for the 2nd, 3rd, and 4th drainage experiments, the outflows measured under quasi-steady-state conditions were used to estimate the lateral saturated soil hydraulic conductivity of the soil blocks, K_{s-SB} (mm h^{-1}), according to Darcy's formula, as follows:

$$K_{s-SB} = -\frac{q}{T}\frac{s}{\Delta Z} \quad (1)$$

where q (L^{2}T^{-1}) is the flow of water per unit width of the block, T (L) is the thickness of the flow zone measured perpendicular to the bed, Z (L) is the water table elevation from an arbitrary datum, and s (L) is the distance measured on a straight line in the direction of the sloping bed. In this investigation, q, T, s, and ΔZ, were measured during the field experiment, or were determined using a simple geometry (**Figure 1**). We decided to use measured inflows rather than outflows only for the first SB1 experiment because: i) field observations during this experiment revealed localized water leakages from the OP and the measured inflow was thus completely infiltrated through the SB1, and ii) the measured inflow of the first experiment was consistent with the other ones.

Di Prima, S., Marrosu, R., Lassabatere, L., Angulo-Jaramillo, R., Pirastru, M., 2018. In situ characterization of preferential flow by combining plot- and point-scale infiltration experiments on a hillslope. Journal of Hydrology 563, 633–642. https://doi.org/10.1016/j.jhydrol.2018.06.033

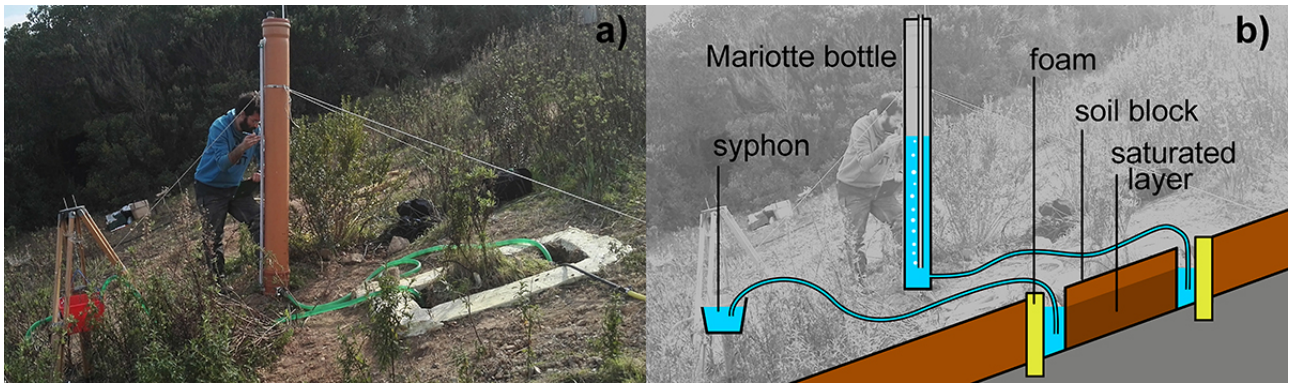

Figure 2. **(a)** Photo and **(b)** schematic view of the experimental setup of a drainage experiment carried out on a soil block.

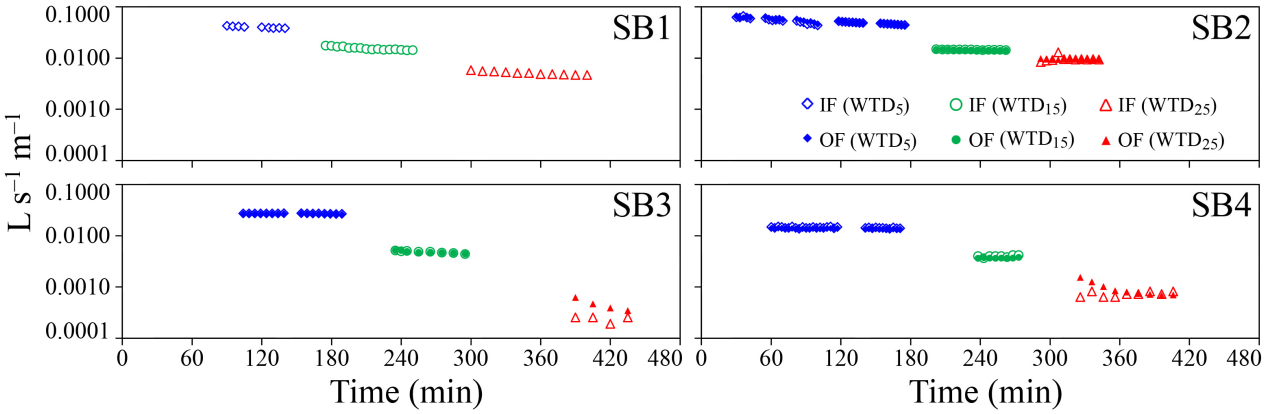

Figure 3. Inflow (IF, open symbols) and outflow (OF, solid symbols) rates vs. time measured on the four soil blocks (SBs) at a water table depth (WTD) of 5 (blue rhombus), 15 (green circles) and 25 cm (red triangles).

2.4. Modified cube method

The horizontal and vertical hydraulic conductivities of the saturated soil, K_s, were determined based on the modified cube method (MCM) (Beckwith et al., 2003) to gain insight on the potential effects of anisotropic conditions on the comparison between the K_s measurements (Blanco-Canqui et al., 2002). In fact, the presence of layers parallel to the soil surface is expected to induce effective horizontal K_s values that are greater than the vertical ones (Zaslavsky and Rogowski, 1969).

According to the procedure described by Bagarello and Sgroi (2008) and Bagarello et al. (2009), a total of 20 soil cubes were collected at depths that ranged between 0–11 cm by carefully carving out 11 cm (width) by 11 cm (length) by 14 cm (depth) soil prisms (**Figure 4a**). A wooden box (side length=17 cm) that was open at the bottom and top sides, was placed around each exposed soil prism (**Figure 4b**). Expandable polyurethane foam was injected between the box and the exposed soil and on the soil surface (**Figure 4c**). To avoid foam adhesion and to facilitate reusing, the box was wrapped with plastic wrap. In order to confine the foam expansion, a wood was positioned on the top of the box (**Figure 4d**). After the total expansion of the foam, the excess was cut off with a knife and the cube was marked to preserve direction. A layer of soil with a 3 cm thickness was removed from the bottom of the prism to obtain a cubic soil sample. Finally, the sample was completely encased by applying the foam at the bottom side.

In the laboratory, the vertical conductivity, $K_{s,v-MCM}$, was measured for ten randomly chosen cubes. The cubes were taken from the wooden box and the foam was removed from the top and bottom faces using a knife. The horizontal conductivity, $K_{s,h-MCM}$, was measured for the remaining soil cubes. In this latter case, the foam was removed from the up and downhill faces of the cube. For each cube, a single measurement was carried out given that the first measurement may affect the second when bidirectional measurements are performed on a single soil cube (Bagarello et al., 2009). A wire net was placed at the bottom face of the cube to support the weight of the soil. The soil samples were then slowly saturated from the bottom for 24 h. The constant-head laboratory permeameter method (Klute and Dirksen, 1986), with an established ponding depth of 1 cm was applied to measure K_s according to Darcy's law. A syphon was used to maintain the constant depth of ponding on the soil surface. The use of a Mariotte bottle with small ponding depths was avoided since it may promote turbulence close to the soil's surface, potentially resulting in clogging the exposed pores (Bagarello et al., 2009). The constant-head permeameter used for measuring $K_{s,v-MCM}$ and $K_{s,h-MCM}$ was operated with water that flowed from the top and the uphill cube faces, respectively. The experiments were

Di Prima, S., Marrosu, R., Lassabatere, L., Angulo-Jaramillo, R., Pirastru, M., 2018. In situ characterization of preferential flow by combining plot- and point-scale infiltration experiments on a hillslope. Journal of Hydrology 563, 633–642. https://doi.org/10.1016/j.jhydrol.2018.06.033

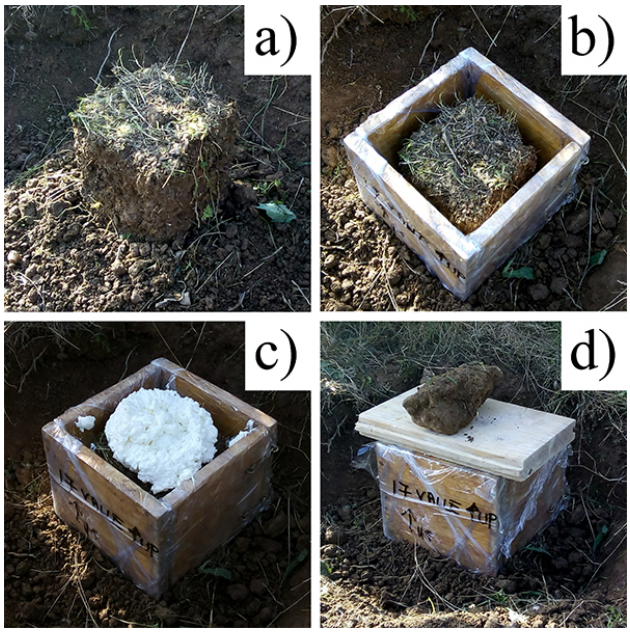

Figure 4. Successive steps during the in situ extraction of the soil cube: **(a)** carving out the soil prism, **(b)** placing the wooden box to contain lateral foam expansion, **(c)** injecting polyurethane expandable foam between the box and the exposed soil and on the soil surface, and **(d)** positioning wood and a weight to prevent top foam expansion.

carried out until steady state conditions were established (i.e., at approximately 30 to 95 min). Depending on the run, the last 10–35 minutes of the measured flow rate data were used to calculate K_s. Finally, for each measurement direction, the ten determinations of K_s were averaged, and the ratio $K_{s,h-MCM}/K_{s,v-MCM}$ was evaluated to check the occurrence of anisotropy, i.e., the prevalence of the vertical ($K_{s,h-MCM}/K_{s,v-MCM} \leq 1$) or horizontal ($K_{s,h-MCM}/K_{s,v-MCM} \geq 1$) flow directions (Beckwith et al., 2003). The chosen sample size (N = 10) was expected to yield representative mean $K_{s,v}$ and $K_{s,l}$ values at the scale considered in this investigation (Reynolds et al., 2002).

2.5. BEST method

The Beerkan estimation of the soil transfer (BEST) parameter method for soil hydraulic characterization introduced by Lassabatere et al. (2006) was chosen for this investigation to yield an estimate for the saturated hydraulic conductivity of the matrix since it constitutes a practical alternative to more cumbersome and time-consuming methods (Bagarello et al., 2014a). Indeed, this method needs simple equipment and minimal field work, and it is gaining popularity in soil science.

A total of 40 ponding infiltration runs of the Beerkan type were carried out at the depths of 0, 5, 10, and 20 cm (ten for each soil depth) at randomly selected points of the hillslope. A small diameter ring (i.e., 8 cm) inserted at a depth of 1 cm was used. The soil disturbance was minimized by the limited ring insertion depth (Alagna et al., 2013). A relatively small ring diameter was chosen since the total sampled area cannot be too large given that the ring had to be inserted on a sloping surface (Angulo-Jaramillo et al., 2016) and to avoid the sampling of the macropore network. For each run, 15 water volumes, each equal to 43 mL, were successively poured on the confined infiltration surface. The number of infiltrated volumes was sufficient to reach steady state, as required by the Beerkan methods (Lassabatere et al., 2006). The energy of the falling water was dissipated with the hand fingers to minimize the soil disturbance owing to water pouring, as commonly suggested (e.g., Alagna et al., 2017; Castellini et al., 2018; Di Prima et al., 2017a; Reynolds, 1993). For each water volume, the time needed for the water to infiltrate was logged, and the cumulative infiltration, I (mm) was plotted against time, t (s). A regression line was then fitted to the last data points to describe the steady-state conditions, to estimate the experimental steady-state infiltration rate, i_s (mm h^{-1}), and the associated intercept, b_s (mm). The steady algorithm of BEST (Bagarello et al., 2014b) was then applied to estimate the saturated soil hydraulic conductivity, K_{s-BEST} (mm h^{-1}) based on the following equation (Di Prima et al., 2016):

$$K_{s-BEST} = \frac{C\, i_s}{A\, b_s + C} \tag{2}$$

where the constants A (mm^{-1}) and C are defined as follows (Haverkamp et al., 1994),

$$A = \frac{\gamma}{r\left(\theta_s - \theta_i\right)} \tag{3a}$$

$$C = \frac{1}{2\left[1 - \left(\frac{\theta_i}{\theta_s}\right)^{\eta}\right]\left(1-\beta\right)} ln\left(\frac{1}{\beta}\right) \tag{3b}$$

where θ_i and θ_s refer to the initial and saturated water contents, respectively, γ (parameter for geometrical correction of the infiltration front shape), and β are the coefficients that are commonly set at 0.75 and 0.6, r (mm) is the radius of the disk source, and η is a shape parameter that is estimated from the analysis of the particle size data with the pedotransfer function included in the BEST procedure (Lassabatere et al., 2006). More details on the methods and the validation of equations based on fitted experimental data can be found in Di Prima et al. (2016) and Lassabatere et al. (2009).

In this investigation, the BEST-steady algorithm was chosen since it yields higher percentage of success (i.e., positive K_s values) on the infiltration runs, and allows simple calculation of K_s as compared to other BEST algorithms, namely BEST-intercept (Yilmaz et al., 2010) and BEST-slope (Lassabatere et al., 2006).

Di Prima, S., Marrosu, R., Lassabatere, L., Angulo-Jaramillo, R., Pirastru, M., 2018. In situ characterization of preferential flow by combining plot- and point-scale infiltration experiments on a hillslope. Journal of Hydrology 563, 633–642. https://doi.org/10.1016/j.jhydrol.2018.06.033

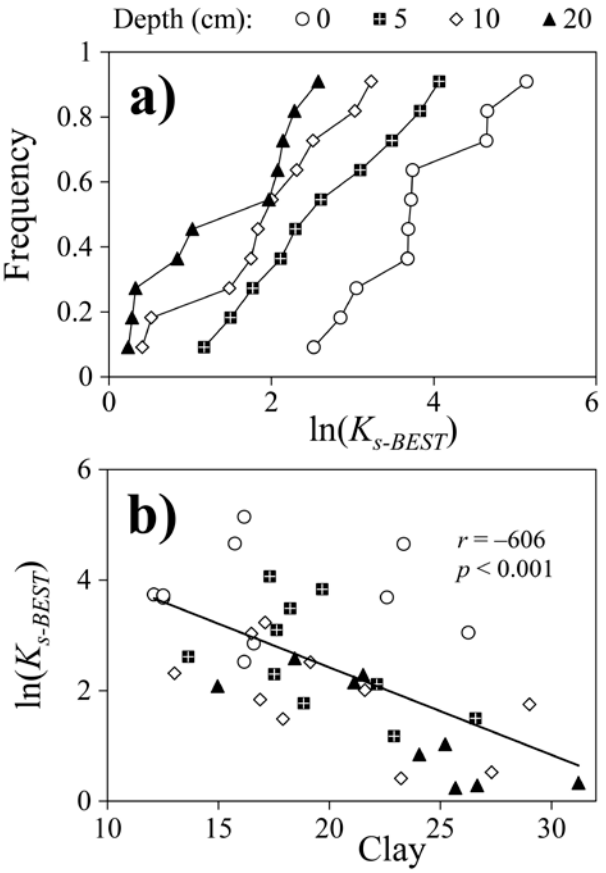

Figure 5. **(a)** Cumulative empirical frequency distributions of the log-transformed saturated soil hydraulic conductivity data, ln($K_{s,BEST}$), obtained by the Beerkan method at the depths of 0, 5, 10, and 20 cm, and **(b)** ln($K_{s–BEST}$) values plotted against the clay content (in %). The Pearson correlation coefficient, *r*, is also reported.

Table 2. Sample size, N, minimum, Min, maximum, Max, geometric mean, m_G, standard deviation, SD, and coefficient of variation, CV (%) of the saturated soil hydraulic conductivity, $K_{s–BEST}$ (mm h^{-1}). All values were obtained using the Beerkan method at the depths of 0, 5, 10, and 20 cm.

Statistic	Depth (cm)			
	0	5	10	20
N	10	10	10	10
Min	12.4	3.2	1.5	1.3
Max	171.1	58.3	25.2	13.2
m_G	43.3 A	13.4 B	6.7 BC	4.0 C
SD	2.3	2.7	2.5	2.5
CV	101.8	130.7	118.8	116.3

The values followed by the same letter were not significantly different according to the Tukey's honest significant difference test ($P < 0.05$). The values followed by a different letter were significantly different.

2.6. Dual-permeability approach

On the basis of the measures obtained from the Beerkan runs and the block method, it was expected that the hydraulic conductivity of macropores would be efficiently computed. For dual permeability systems, it is considered that the global hydraulic conductivity, $K_{s,2K}$ (mm h^{-1}), can be decoupled in terms of its contributions to the matrix and to the fast-flow region (Gerke and van Genuchten, 1993),

$$K_{s,2K} = w_f K_{s,f} + (1 - w_f) K_{s,m} \quad (4)$$

where w_f is the void ratio occupied by the fast-flow region (dimensionless), i.e., the ratio of the volumes of the macropore and total-flow regions, and $K_{s,f}$ and $K_{s,m}$ (mm h^{-1}) are the saturated hydraulic conductivities for the fast-flow and the matrix regions, respectively. In this investigation, we assumed that we had an estimate for the saturated hydraulic conductivity of the matrix from the Beerkan runs. If we also assume that $K_{s,2K}$ can be estimated by the bulk values obtained based on drainage experiments, we can deduce the hydraulic conductivity of the fast-flow region using equation (4), and its solution for $K_{s,f}$, which leads to,

$$K_{s,f} = \frac{K_{s,2K} - (1 - w_f) K_{s,m}}{w_f} \quad (5)$$

Since the void ratio occupied by the fast-flow region was unknown, we have evaluated multiple scenarios with w_f values ranging from 0.05 to 0.1, i.e., the fast-flow region was considered to occupy 5 to 10% of the entire region. This range was adopted since the fast-flow fraction generally occupied a very small fraction of the soil's porosity (Bouma et al., 1977). Moreover, these values were selected to agree with those reported by many dual-permeability applications. For instance, Dusek et al. (2012) settled the w_f values to 7% and 5% at the soil surface and at a 75 cm depth, respectively, in a hillslope covered with grass (Calamagrostis villosa) and spruce (Picea abies). For numerical simulations, Lassabatere et al. (2014b) considered a value of 10% for w_f.

2.7. Data analyses

K_s data were assumed to be log-normally distributed since the statistical distribution of these data is generally log-normal (Lee et al., 1985; Warrick, 1998). Therefore, the geometric mean, m_G, and the associated standard deviation, SD, and coefficient of variation, CV, were calculated using the appropriate "log-normal Equations" (Lee et al., 1985). The arithmetic mean, m_A, was calculated for ρ_b, θ_i, and θ_s. Statistical comparison between the two sets of data was conducted using two-tailed Student's *t*-tests, whereas the Tukey's honestly significant test was applied to compare three or more datasets. The ln(K_s) data were considered for comparative purposes since K_s was better described by the log-normal distribution than the normal distribution. An updated version of the workbook by Di Prima (2013) was used to analyze the Beerkan infiltration runs by the BEST-steady algorithm. All statistical analyses were carried out using the Minitab© computer program (Minitab Inc., State College, PA, USA).

Di Prima, S., Marrosu, R., Lassabatere, L., Angulo-Jaramillo, R., Pirastru, M., 2018. In situ characterization of preferential flow by combining plot- and point-scale infiltration experiments on a hillslope. Journal of Hydrology 563, 633–642. https://doi.org/10.1016/j.jhydrol.2018.06.033

Table 3. Sample size, N, minimum, Min, maximum, Max, geometric mean, m_G, standard deviation, SD, and coefficient of variation, CV (%) of the vertical, $K_{s,v-MCM}$ (mm h^{-1}) and horizontal, $K_{s,h-MCM}$ (mm h^{-1}) saturated soil hydraulic conductivity values obtained by the constant-head laboratory permeameter method on soil cubes (Klute and Dirksen, 1986).

$m_G(K_{s,h-MCM})/m_G(K_{s,v-MCM})$	Statistic	$K_{s,v-MCM}$	$K_{s,h-MCM}$
0.97	N	10	10
	Min	51.7	52.6
	Max	480.7	341.4
	m_G	173.0 A	167.1 A
	SD	2.1	1.9
	CV	87.5	71.9

The two K_s values followed by the same letter are not significantly different according to a Student's two-tailed *t*-test ($P < 0.05$).

3. Results and discussion

3.1. In-situ and laboratory small-scale measurements

Our results show that the K_s values estimated with the Beerkan method (K_{s-BEST}) progressively decreased with soil depth (**Figure 5a** and **Table 2**). From a statistical point-of-view, results of the Tukey's honestly significant difference test showed significant differences between the K_s values measured at different soil depths. The dry soil bulk density, ρ_b, ranged between 1.44 and 1.78 g cm^{-3} (N = 12). No differences were detected along the soil profile in terms of ρ_b (**Table 1**). Conversely, the K_{s-BEST} values increased with the sand content (Pearson's correlation coefficients, r = 0.471; p = 0.002) and decreased with the clay content (r = –0.606; $p < 0.001$, **Figure 5b**). The higher percentage of coarse particles in the upper soil layer could suggest a certain rigidity of the porous medium (**Table 1**). On the contrary, the increase in clay particles with soil depth implies more opportunities for clogging the largest pores, and thus, lower K_s values. In the upper soil, these values were very close to the prediction of saturated conductivity from soil textural characteristics (e.g., K_s = 44.2 mm h^{-1} for a sandy–loam soil according to Carsel and Parrish (1988)). Therefore, the macroporosity did not likely influence the measured infiltration process. In general, isolated macropores are physically difficult to include in the sampled volume (Brooks et al., 2004). Using small rings in the soils with macropores (with ring inner diameters of 8 cm in this investigation) implies a relatively high probability to sample only the soil matrix. This yields a measurement of K_s that is representative only of the matrix instead of the entire system of macropores (Angulo-Jaramillo et al., 2016). In addition, using small rings also implies fewer opportunities of inclusion of continuous macropores intersecting the confined soil surface. Large rings appear more appropriate than small rings in eliciting a signal associated with the occurrence of soil macropores or fast-flow regions in the field since smaller soil volumes are functionally more homogeneous than larger volumes (Bagarello et al., 2013). Castellini et al. (2016) applied the Beerkan method using a ring with an inner diameter of 15 cm to assess the physical quality of the upper soil of the same experimental hillslope. These authors obtained similar results for K_s (mean = 24.1 mm h^{-1}, coefficient of variation, CV = 118). The mean K_s values collected during the two sampling campaigns differed by a factor of 1.8. This could be considered practically negligible for many hydrological applications (Elrick and Reynolds, 1992).

Table 3 summarizes the parameters obtained by the modified cube method (MCM). The means of K_s were equal to 173.0 and 167.1 mm h^{-1} for the vertical and horizontal directions, respectively. The MCM yielded statistically different and higher K_s estimates than Beerkan. The comparison between these methods requires additional considerations that are discussed below. In-situ K_s measurements allow the maintenance of the functional connections of the sampled volumes with the surrounding matrix (e.g., Bagarello et al., 2017; Bouma, 1982; Di Prima, 2015; Lauren et al., 1988). In comparison, in the laboratory, the overall connection of extracted soil samples is expected to be higher because of the increased probability of their impact by macropores and the interception of the edges of the extracted samples. We thus conclude that the higher values of saturated hydraulic conductivity for the MCM method results from a partial activation of the largest pores in the soil samples. This increase in connectivity was discussed in detail in a review article by Pachepsky and Hill (2017). To explain this effect, these authors considered data from one-dimensional vertical water flow experiments. In these experiments, K_s decreased with increases of the soil column length L according to the following power law $K_s \propto L^{-m}$. Anderson and Bouma (1973) attributed this effect to the increasing probability that pores will remain connected throughout the length of a core as a function of decreasing core lengths. In particular, for longer samples, the water flux appears to be controlled by a more homogeneous soil matrix with lower hydraulic conductivity values. The process discussed above essentially mimics what happens during the Beerkan infiltration runs, which allow the preservation of the functional connection of the sampled volume with the surrounding matrix, thus yielding lower K_s values than those obtained with the MCM (samples biased by pores).

Several examples of the overestimation of K_s on extracted soil samples can be found in the literature. For instance, the increase in K_s owing to open-ended pores on undisturbed soil samples was assessed by Blanco–Canqui et al. (2002). These authors measured K_s on 180 soil cores (with 76 mm (diameter) × 76 mm (height)) with and without bentonite to seal the macropores. These authors found that K_s values without bentonite were approximately four times higher than the corresponding K_s values with bentonite. Kanwar et al. (1989) compared the K_s values determined in situ using the Guelph permeameter device (Reynolds and Elrick, 2005) and the velocity permeameter (Merva, 1979) with those obtained in the laboratory based on the constant head permeameter method on undisturbed soil cores (75 mm (diameter) × 75 mm (height)). The in situ methods yielded values that were 10–800 times lower than the laboratory method. Young (1998) and Regan

Di Prima, S., Marrosu, R., Lassabatere, L., Angulo-Jaramillo, R., Pirastru, M., 2018. In situ characterization of preferential flow by combining plot- and point-scale infiltration experiments on a hillslope. Journal of Hydrology 563, 633–642. https://doi.org/10.1016/j.jhydrol.2018.06.033

Table 4. Geometrical dimensions and estimated saturated hydraulic conductivity, K_{s-SB} (mm h^{-1}) values for the four soil blocks.

	Depth (cm)	Length (cm)	Width (cm)	Volume (m^3)	K_{s-SB}		
					WTD_5	WTD_{15}	WTD_{25}
Soil block 1	35.5	85	54.0	0.163	1.4×10^{3}	7.9×10^{2}	5.1×10^{2}
Soil block 2	29.0	69	50.0	0.100	2.2×10^{3}	1.2×10^{3}	2.8×10^{3}
Soil block 3	30.0	68	50.0	0.102	1.1×10^{3}	3.1×10^{2}	7.0×10^{1}
Soil block 4	31.5	80	52.5	0.132	7.2×10^{2}	3.1×10^{2}	1.5×10^{2}
m_G					1.2×10^{3}	5.5×10^{2}	3.5×10^{2}
Mean	31.5	75.5	51.6	0.124			
SD	2.9	8.3	2.0	0.030	1.6	2.0	5.0
CV (%)	9.1	11.1	3.8	23.9	48.6	76.3	345.8

(2000) measured K_s values using vertical soil cores and the Guelph permeameter, respectively. The in situ methods yielded values that were three to four times lower than the soil core K_s measurements. Differences were attributed to continuous pores connecting the exposed surfaces of the cores for the laboratory method.

In this investigation, the soil cube method provided further insight on the potential effect of anisotropic conditions on the comparison between K_s measurements (Blanco–Canqui et al., 2002). The anisotropy of K_s was not substantial given that the difference between the $K_{s,v-MCM}$ and $K_{s,h-MCM}$ values was not statistically significant, according to a two-tailed Student's *t*-test ($P < 0.05$) (Dabney and Selim, 1987). The ratio between the mean values of $K_{s,v-MCM}$ and $K_{s,h-MCM}$ was equal to 0.97 (**Table 3**). In general, the effect of allowing only one-dimensional flow into the soil leads to an important "error" when the anisotropy is large and when no attempt is made to measure separately the horizontal and vertical components of permeability (Chappell and Lancaster, 2007). However, the biasing problem on small soil cubes and the impossibility to sample all the macropores probably precluded the detection of the effect that macropores may exert on a specific flow direction. Indeed, even if we explained the higher values of the MCM method in comparison to Beerkan estimates obtained on the field based on the hypothesis of the activation of the macropore network, we are not sure that this activation is complete. In addition, the size of the soil samples may not be large enough to sample the largest macropores encountered in the field. In other words, the measurement of the vertical and horizontal flow on small soil cubes may not be representative of the real anisotropic behavior of the macropore network that may occur at a larger scale in the field. However, we can consider that for the matrix alone, the runs are representative of the field conditions. Therefore, the result of a substantial isotropic behavior of the soil at the point scale suggested that the direction of the flow measurements, i.e., vertical or horizontal, did not play a role on K_s estimation for the matrix at the small scale.

3.2. Comparing plot- and point-scale measurements

Figure 3 shows the subsurface flows measured for three different water table depths (WTDs) for the four soil blocks. The steady flow rates ranged from 3.4×10^{-4} to 4.4×10^{-2} L s^{-1} m^{-1} (sample size, $N = 12$), thus yielding K_{s-SB} values that equaled 70 and 2157 mm h^{-1} (**Table 4**) for WTD_{25} and WTD_5, respectively. For WTD_5, the mean K_{s-SB} value (1239 mm h^{-1}, sample size, $N = 4$) was an order of magnitude higher than that elicited by the MCM. Therefore, a smaller soil volume was found to be more homogeneous than a larger volume (Lai and Ren, 2007). Macropore flow likely occurred at the sampled site since even the lowest mean of K_{s-SB} (724 mm h^{-1}) was 4.3 times higher than those of the MCM, known to overestimate the saturated hydraulic conductivity of the matrix (see discussion above). The discrepancy between the two spatial scales is even greater for the case of the Beerkan runs. Therefore, both laboratory and small-scale field measurements yielded consistently lower values than those of the plot-scale. Small-scale measurements also yielded higher standard deviations (SDs) and coefficient of variations (CVs) than those obtained on the soil blocks for WTD_5, thus suggesting the degradation of sample representativeness at smaller scales. In fact, the variability of the data is expected to decrease as the size of the sampled soil volume increases (Angulo-Jaramillo et al., 2016). Conversely, large soil volumes allowed the determination of representative K_{s-SB} values that account for soil heterogeneity and the contribution of the macropore network. This result is also consistent with the suggestion of Pachepsky and Hill (2017) who stated that the macropore flow cannot be seen at the small scale but emerges and becomes of interest at the plot scale. In other words, the large volume of soil adequately embodied the macropore network (Blanco-Canqui et al., 2002; Day et al., 1998; Mendoza and Steenhuis, 2002). The relatively low variability of the data (CV = 48.6%) also suggested the replicability of the measurements.

3.3. Lateral preferential flow

The results from the comparison between plot- and point-scale measurements suggested that the studied soil was clearly made of two components, namely, the matrix and the macropore network that constituted a fast-flow region. In the following subsection, we attempt to fully characterize both regions. The matrix could be characterized by the values of saturated hydraulic conductivity obtained with Beerkan runs. The Beerkan runs along with the four drainage experiments were used to estimate the saturated hydraulic conductivity of

Di Prima, S., Marrosu, R., Lassabatere, L., Angulo-Jaramillo, R., Pirastru, M., 2018. In situ characterization of preferential flow by combining plot- and point-scale infiltration experiments on a hillslope. Journal of Hydrology 563, 633–642. https://doi.org/10.1016/j.jhydrol.2018.06.033

Table 5. Estimated values of the saturated hydraulic conductivity for the fast-flow region, $K_{s,f}$ (mm h^{-1}), for the lower (0.05) and upper (0.1) range values of the void ratio occupied by the fast-flow region, w_f (-), for the four soil blocks.

	$K_{s,f}$ (w_f = 0.05)			$K_{s,f}$ (w_f = 0.1)		
	WTD_5	WTD_{15}	WTD_{25}	WTD_5	WTD_{15}	WTD_{25}
Soil block 1	2.8×10^4	1.6×10^4	10.0×10^3	1.4×10^4	7.8×10^3	5.0×10^3
Soil block 2	4.3×10^4	2.3×10^4	5.5×10^4	2.1×10^4	1.2×10^4	2.7×10^4
Soil block 3	2.1×10^4	5.9×10^3	1.2×10^3	1.1×10^4	3.0×10^3	6.0×10^2
Soil block 4	1.4×10^4	6.0×10^3	2.8×10^3	7.1×10^3	3.0×10^3	1.4×10^3
m_G	2.5×10^4	1.1×10^4	6.5×10^3	1.2×10^4	5.4×10^3	3.3×10^3
SD	1.6	2.0	5.3	1.6	2.0	5.3
CV (%)	49.1	78.3	387.5	49.1	78.2	385.0

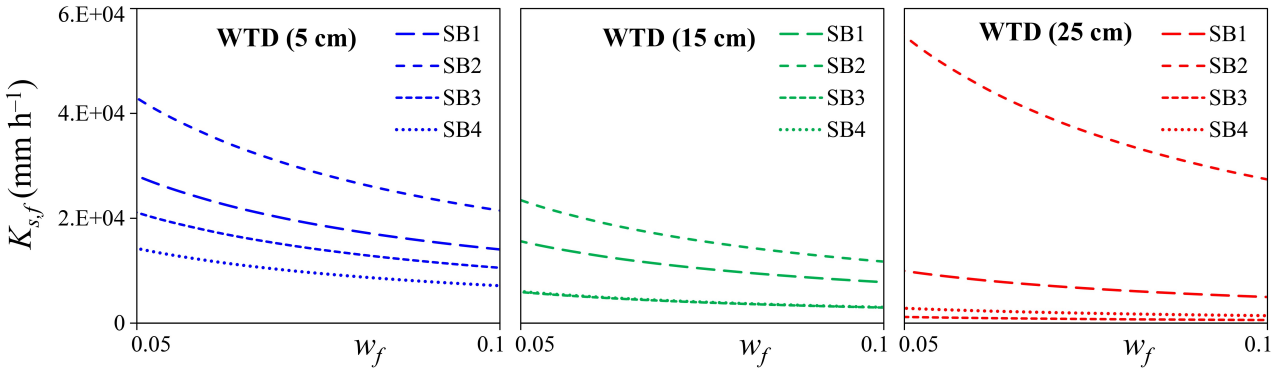

Figure 6. Impact of the fast-flow fraction, w_f (-), on the saturated hydraulic conductivity for the fast-flow region, $K_{s,f}$ (mm h^{-1}), estimated at different water table depths (WTDs) on the four soil blocks (SBs). The reported w_f values range from 0.05 to 0.1.

the fast-flow region, $K_{s,f}$ (mm h^{-1}) using Eq. (5). The values of $K_{s,f}$ ranged from 6.0×10^2 to 5.5×10^4 mm h^{-1}, depending on the WTD and w_f values (**Table 5**). For the lower (0.05) and upper (0.1) range values of w_f, the $K_{s,f}$ estimates were in the range of two to three and one to three orders of magnitude higher than $K_{s,m}$, respectively. Conversely, differences never exceeding a factor of two were encountered for the $K_{s,f}$ estimates within the selected w_f ranges, which may be considered within the natural range of spatial heterogeneity for the saturated hydraulic conductivity (Kodešová et al., 2010). Therefore, because larger discrepancies occurred between the fast-flow and the matrix regions, it can be argued that the selected w_f values had a lesser impact on the comparison between the K_m and K_f values.

Figure 6 shows the impact of w_f on the $K_{s,f}$ values estimated at different water table depths (WTDs) for the four soil blocks. Firstly, it should be taken into account that the global hydraulic conductivity was measured in the field, and thus Eq. (5) was applied constraining $K_{s,2k}$ values. As shown in **Figure 6**, $K_{s,f}$ estimates decreased for higher w_f values. To explain this general trend, we should consider that with the constrained $K_{s,2k}$ value, the increase of w_f should correspond to a decrease in $K_{s,f}$ estimates. Indeed, the product of w_f $K_{s,f}$ that quantifies the contribution of the macropore network to the bulk hydraulic conductivity $K_{s,2K}$ (Eq.(4)) must remain constant irrespective of the value of w_f. This condition is representative of a larger volume occupied by macropores, which are in turn less connected, and/or with a smaller diameter corresponding to lower hydraulic conductivities. On the contrary, when w_f decreases, the increase in $K_{s,f}$ is representative of a smaller volume occupied by more connected and/or larger diameter macropores and a higher hydraulic conductivity. In any case, the contribution of the macropore network system remains constant. Moreover, $K_{s,f}$ estimates decreased for higher WTDs, i.e., for a thinner saturated soil layer, with the exception of soil block 2. In this case, a higher $K_{s,f}$ value was estimated for WTD_{25} because of the effect of an open-ended macropore biasing the matrix that was located at the bottom of the soil block. This hypothesis was supported by field observations. In particular, during the saturation stage, we observed water copiously flowing from a deep macropore. This contributed to a higher $K_{s,f}$ value than those obtained for lower WTDs. However, as shown in **Figure 6**, the overall decrease of $K_{s,f}$ supported the hypothesis that the macropore density decreased with depth. It can be argued that the sampled volume should be increased for lower horizons in order to adequately represent the macropore network. In contrast, the increase in WTD from 5 to 15 and to 25 cm resulted in a reduction of the sampled soil volume. Under such conditions, the sampled volumes may have not been sufficient to activate the macropore networks located in the deeper horizons. Moreover, the $K_{s,f}$ variability increased abruptly for thinner saturated layers. A smaller macropore density was noted as a function of depth that increased the macropore flow variability, which may ultimately contribute to the explanation of the smaller transfer rates in the deeper horizons (Köhne et al., 2009).

These results implied that the proper scale to study macropore flow for small thickness of the saturated layer may be the hillslope-scale on the studied hillslope. This effect likely had a certain impact on the measurements for lower WTDs, thus resulting in a minor $K_{s,f}$ overestimation in some

Di Prima, S., Marrosu, R., Lassabatere, L., Angulo-Jaramillo, R., Pirastru, M., 2018. In situ characterization of preferential flow by combining plot- and point-scale infiltration experiments on a hillslope. Journal of Hydrology 563, 633–642. https://doi.org/10.1016/j.jhydrol.2018.06.033

circumstances owing to the occasional presence of deep, open-ended macropores (soil block 2). Notwithstanding this finding, considering the entire volume of the soil blocks, the water flow was mainly controlled by the dense macropore network which characterized the porous medium in proximity of the soil surface. Thus, in these cases, the effect of deep, open-ended macropores, was less noticeable.

4. Conclusions

This investigation was carried out to characterize the subsurface flow processes in a hillslope at different spatial scales, namely at point- and plot-scale using the Beerkan method with the BEST algorithm, the MCM, and the soil block method. The differences between the considered scales were attributed mainly to the effect of the macropore flow and the impossibility to adequately embody the macropore network on small sampled soil volumes. The comparison of K_s measurement techniques allowed us to establish the peculiarity of each K_s data obtained at a particular spatial scale. This information helped establish the usability of a given technique to interpret or simulate a particular hydrological process. In particular, the scale dependence of K_s essentially precluded the use of small-scale measurements for detecting a dual-permeability behavior. Otherwise, plot-scale measurements allowed us to obtain reliable estimates accounting for macropore flow. In our study, we clearly proved the advantage of experimental protocols based on multiscale experiments. Our results yielded encouraging evidence for the applicability of the soil block method (at the plot-scale) along the Beerkan infiltration runs (at the point-scale) for a plausible estimation of the saturated hydraulic conductivities for the matrix and the fast-flow region, $K_{s,m}$ and $K_{s,f}$, using a relatively simple field procedure. The use of expandable polyurethane foam as a suitable material to encase soil blocks for hydraulic conductivity measurements was successfully tested. It closely adhered to the irregular soil surface (Brye et al., 2004; Germer and Braun, 2015; Muller and Hamilton, 1992), avoided water loss and obtained accurate measurements of K_s. This is a promising result given that researcher studies should constantly focus their efforts to simplify field measurements (Alagna et al., 2016).

In the future, the proposed methodology may be applied to explain saturation excess runoff (i.e., saturation overland flow) or to study subsurface macropore flow. Indeed, these processes constitute the major mechanisms affecting the dynamics of the shallow groundwater perched table above a restrictive layer, which is an integrated process that needs a minimum contributing area to be activated (Blöschl and Sivapalan, 1995). Further experimental work is needed to determine the macropore domain (w_f). Based on this aim, the fraction of the macropore domain in the dual-permeability model could be estimated using micromorphological images (Kodešová et al., 2009). This approach could allow us to estimate w_f as the ratio of the porosity determined by image analysis and the overall porosity of the sampled soil. The role of the macropores in controlling $K_{s,f}$ at the studied hillslope needs to be further investigated. For example, tracer experiments may be carried out to investigate macroporosity extensions and connectivity (Ahuja et al., 1995; Köhne et al., 2009), which was considered responsible for the detected scale dependence of the studied soil properties.

Acknowledgements

This work was supported through the progetto Legge 7 (LR72013UNICANIEDDA) “Impatti antropogenici e climatici sul ciclo idrogeologico a scala di bacino e di versante” (“Anthropogenic and climate impacts affecting the hydrological cycle at the hillslope and catchment scales”).

References

Abou Najm, M.R., Atallah, N.M., 2016. Non-Newtonian Fluids in Action: Revisiting Hydraulic Conductivity and Pore Size Distribution of Porous Media. Vadose Zone Journal 15, 0. https://doi.org/10.2136/vzj2015.06.0092

Ahuja, L.R., Johnsen, K.E., Heathman, G.C., 1995. Macropore Transport of a Surface-Applied Bromide Tracer: Model Evaluation and Refinement. Soil Science Society of America Journal 59, 1234–1241. https://doi.org/10.2136/sssaj1995.03615995005900050004x

Akay, O., Fox, G.A., Šimůnek, J., 2008. Numerical Simulation of Flow Dynamics during Macropore–Subsurface Drain Interactions Using HYDRUS. Vadose Zone Journal 7, 909. https://doi.org/10.2136/vzj2007.0148

Alagna, V., Bagarello, V., Di Prima, S., Giordano, G., Iovino, M., 2013. A simple field method to measure the hydrodynamic properties of soil surface crust. Journal of Agricultural Engineering 44, 74–79. https://doi.org/10.4081/jae.2013.(s1):e14

Alagna, V., Bagarello, V., Di Prima, S., Iovino, M., 2016. Determining hydraulic properties of a loam soil by alternative infiltrometer techniques. Hydrological Processes 30, 263–275. https://doi.org/10.1002/hyp.10607

Alagna, V., Di Prima, S., Rodrigo-Comino, J., Iovino, M., Pirastru, M., Keesstra, S.D., Novara, A., Cerdà, A., 2017. The Impact of the Age of Vines on Soil Hydraulic Conductivity in Vineyards in Eastern Spain. Water 10, 14. https://doi.org/10.3390/w10010014

Anderson, J.L., Bouma, J., 1973. Relationships Between Saturated Hydraulic Conductivity and Morphometric Data of an Argillic Horizon. Soil Science Society of America Journal 37, 408–413. https://doi.org/10.2136/sssaj1973.03615995003700030029x

Angulo-Jaramillo, R., Bagarello, V., Iovino, M., Lassabatère, L., 2016. Infiltration Measurements for Soil Hydraulic Characterization. Springer International Publishing.

Bagarello, V., Di Prima, S., Giordano, G., Iovino, M., 2014a. A test of the Beerkan Estimation of Soil Transfer parameters (BEST) procedure. Geoderma 221–222, 20–27. https://doi.org/10.1016/j.geoderma.2014.01.017

Bagarello, V., Di Prima, S., Iovino, M., 2017. Estimating saturated soil hydraulic conductivity by the near steady-state phase of a Beerkan infiltration test. Geoderma 303, 70–77. https://doi.org/10.1016/j.geoderma.2017.04.030

Bagarello, V., Di Prima, S., Iovino, M., 2014b. Comparing Alternative Algorithms to Analyze the Beerkan Infiltration Experiment. Soil Science Society of America Journal 78, 724. https://doi.org/10.2136/sssaj2013.06.0231

Bagarello, V., Iovino, M., Lai, J.-B., 2013. Field and Numerical Tests of the Two-Ponding Depth Procedure for Analysis of Single-Ring Pressure Infiltrometer Data. Pedosphere 23, 779–789. https://doi.org/10.1016/S1002-0160(13)60069-7

Bagarello, V., Sferlazza, S., Sgroi, A., 2009. Testing laboratory methods to determine the anisotropy of saturated hydraulic conductivity in a sandy–loam soil. Geoderma 154, 52–58. https://doi.org/10.1016/j.geoderma.2009.09.012

Bagarello, V., Sgroi, A., 2008. Testing Soil Encasing Materials for Measuring Hydraulic Conductivity of a Sandy-Loam Soil by the Cube Methods. Soil Science Society of America Journal 72, 1048. https://doi.org/10.2136/sssaj2007.0022

Beckwith, C.W., Baird, A.J., Heathwaite, A.L., 2003. Anisotropy and depth-related heterogeneity of hydraulic conductivity in a bog peat. I: laboratory measurements. Hydrol. Process. 17, 89–101. https://doi.org/10.1002/hyp.1116

Beven, K., Germann, P., 1982. Macropores and water flow in soils. Water Resour. Res. 18, 1311–1325. https://doi.org/10.1029/WR018i005p01311

Blanco-Canqui, H., Gantzer, C.J., Anderson, S.H., Alberts, E.E., Ghidey, F., 2002. Saturated hydraulic conductivity and its impact on simulated runoff for claypan soils. Soil Science Society of America Journal 66, 1596. https://doi.org/10.2136/sssaj2002.1596

Blöschl, G., Sivapalan, M., 1995. Scale issues in hydrological modelling: a review. Hydrological processes 9, 251–290.

Bouma, J., 1982. Measuring the hydraulic conductivity of soil horizons with continuous macropores. Soil Science Society of America Journal 46, 438. https://doi.org/10.2136/sssaj1982.03615995004600020047x

Bouma, J., Jongerius, A., Boersma, O., Jager, A., Schoonderbeek, D., 1977. The function of different types of macropores during saturated flow through four swelling soil horizons. Soil Science Society of America Journal 41, 945–950.

Brooks, E.S., Boll, J., McDaniel, P.A., 2004. A hillslope-scale experiment to measure lateral saturated hydraulic conductivity. Water Resour. Res. 40, W04208. https://doi.org/10.1029/2003WR002858

Brye, K.R., Morris, T.L., Miller, D.M., Formica, S.J., Eps, V., A, M., 2004. Estimating Bulk Density in Vertically Exposed Stoney Alluvium Using a Modified Excavation Method. Journal of Environmental Quality 33, 1937–1942. https://doi.org/10.2134/jeq2004.1937

Carsel, R.F., Parrish, R.S., 1988. Developing joint probability distributions of soil water retention characteristics. Water Resour. Res. 24, 755–769. https://doi.org/10.1029/WR024i005p00755

Castellini, M., Di Prima, S., Iovino, M., 2018. An assessment of the BEST procedure to estimate the soil water retention curve: A comparison with the evaporation method. Geoderma 320, 82–94. https://doi.org/10.1016/j.geoderma.2018.01.014

Castellini, M., Iovino, M., Pirastru, M., Niedda, M., Bagarello, V., 2016. Use of BEST Procedure to Assess Soil Physical Quality in the Baratz Lake Catchment (Sardinia, Italy). Soil Science Society of America Journal 0, 0. https://doi.org/10.2136/sssaj2015.11.0389

Chappell, N.A., Lancaster, J.W., 2007. Comparison of methodological uncertainties within permeability measurements. Hydrological Processes 21, 2504–2514. https://doi.org/10.1002/hyp.6416

Chapuis, R.P., Dallaire, V., Marcotte, D., Chouteau, M., Acevedo, N., Gagnon, F., 2005. Evaluating the hydraulic conductivity at three different scales within an unconfined sand aquifer at Lachenaie, Quebec. Canadian Geotechnical Journal 42, 1212–1220. https://doi.org/10.1139/t05-045

Dabney, S.M., Selim, H.M., 1987. Anisotropy of a Fragipan Soil: Vertical vs. Horizontal Hydraulic Conductivity1. Soil Science Society of America Journal 51, 3. https://doi.org/10.2136/sssaj1987.03615995005100010001x

Day, R.L., Calmon, M.A., Stiteler, J.M., Jabro, J.D., Cunningham, R.L., 1998. Water balance and flow patterns in a fragipan using in situ soil block. Soil science 163, 517–528.

Di Prima, S., 2015. Automated single ring infiltrometer with a low-cost microcontroller circuit. Computers and Electronics in Agriculture 118, 390–395. https://doi.org/10.1016/j.compag.2015.09.022

Di Prima, S., 2013. Automatic analysis of multiple Beerkan infiltration experiments for soil Hydraulic Characterization, in: 1st CIGR Inter-Regional Conference on Land and Water Challenges. p. 127. https://doi.org/10.13140/2.1.4112.0324

Di Prima, S., Bagarello, V., Lassabatere, L., Angulo-Jaramillo, R., Bautista, I., Burguet, M., Cerdà, A., Iovino, M., Prosdocimi, M., 2017a. Comparing Beerkan infiltration tests with rainfall simulation experiments for hydraulic characterization of a sandy-loam soil. Hydrological Processes 31, 3520–3532. https://doi.org/10.1002/hyp.11273

Di Prima, S., Lassabatere, L., Bagarello, V., Iovino, M., Angulo-Jaramillo, R., 2016. Testing a new automated single ring infiltrometer for Beerkan infiltration experiments. Geoderma 262, 20–34. https://doi.org/10.1016/j.geoderma.2015.08.006

Di Prima, S., Marrosu, R., Pirastru, M., Bagarello, V., Iovino, M., Niedda, M., 2017b. In situ determination of the lateral soil hydraulic conductivity on a soil monolith, in: 11th AIIA 2017 Conference - Biosystems Engineering Addressing the Human Challenges of the 21st Century, Bari – Italy, 5-8 July 2017.

Di Prima, S., Rodrigo-Comino, J., Novara, A., Iovino, M., Pirastru, M., Keesstra, S., Cerda, A., 2018. Assessing soil physical quality of citrus orchards under tillage, herbicide and organic managements. Pedosphere 28(3).

Dusek, J., Vogel, T., Dohnal, M., Gerke, H.H., 2012. Combining dual-continuum approach with diffusion wave model to include a preferential flow component in hillslope scale modeling of shallow subsurface runoff. Advances in Water Resources 44, 113–125. https://doi.org/10.1016/j.advwatres.2012.05.006

Elrick, D.E., Reynolds, W.D., 1992. Methods for analyzing constant-head well permeameter data. Soil Science Society of America Journal 56, 320. https://doi.org/10.2136/sssaj1992.03615995005600010052x

Gee, G.W., Bauder, J.W., 1986. Particle-size Analysis, in: SSSA Book Series, Klute, A. (Ed.), Methods of Soil Analysis, Part 1: Physical and Mineralogical Methods. Soil Science Society of America, American Society of Agronomy, pp. 383–411.

Gerke, K.M., Sidle, R.C., Mallants, D., 2015. Preferential flow mechanisms identified from staining experiments in forested hillslopes: Preferential Flow Mechanisms Identified from Staining Experiments. Hydrological Processes 29, 4562–4578. https://doi.org/10.1002/hyp.10468

Gerke, H.H., van Genuchten, M.T., 1993. A dual-porosity model for simulating the preferential movement of water and solutes in structured porous media. Water Resour. Res. 29, 305–319. https://doi.org/10.1029/92WR02339

Germer, K., Braun, J., 2015. Determination of Anisotropic Saturated Hydraulic Conductivity of a Macroporous Slope Soil. Soil Science Society of America Journal 79, 1528–1536. https://doi.org/10.2136/sssaj2015.02.0071

Groppelli, B., Soncini, A., Bocchiola, D., Rosso, R., 2011. Evaluation of future hydrological cycle under climate change scenarios in a mesoscale Alpine watershed of Italy. Nat. Hazards Earth Syst. Sci. 11, 1769–1785. https://doi.org/10.5194/nhess-11-1769-2011

Haverkamp, R., Bouraoui, F., Zammit, C., Angulo-Jaramillo, R., 1999. Soil properties and moisture movement in the unsaturated zone. Handbook of groundwater engineering.

Haverkamp, R., Ross, P.J., Smettem, K.R.J., Parlange, J.Y., 1994. Three-dimensional analysis of infiltration from the disc infiltrometer: 2. Physically based infiltration equation. Water Resour. Res. 30, 2931–2935. https://doi.org/10.1029/94WR01788

Kanwar, R.S., Rizvi, H.A., Ahmed, M., Horton, R., Marley, S.J., 1989. Measurement of field-saturated hydraulic conductivity by using Guelph and velocity permeameters. Transactions of the ASAE 132.

Klute, A., Dirksen, C., 1986. Hydraulic Conductivity and Diffusivity: Laboratory Methods. Methods of Soil Analysis: Part 1—Physical and Mineralogical Methods sssabookseries, 687–734. https://doi.org/10.2136/sssabookser5.1.2ed.c28

Kodešová, R., Šimůnek, J., Nikodem, A., Jirků, V., 2010. Estimation of the Dual-Permeability Model Parameters using Tension Disk Infiltrometer and Guelph Permeameter. Vadose Zone Journal 9, 213. https://doi.org/10.2136/vzj2009.0069

Kodešová, R., Vignozzi, N., Rohošková, M., Hájková, T., Kočárek, M., Pagliai, M., Kozák, J., Šimůnek, J., 2009. Impact of varying soil structure on transport processes in different diagnostic horizons of three soil types. Journal of Contaminant Hydrology 104, 107–125. https://doi.org/10.1016/j.jconhyd.2008.10.008

Köhne, J.M., Köhne, S., Šimůnek, J., 2009. A review of model applications for structured soils: a) Water flow and tracer transport.

Journal of Contaminant Hydrology 104, 4–35. https://doi.org/10.1016/j.jconhyd.2008.10.002
Lai, J., Ren, L., 2007. Assessing the Size Dependency of Measured Hydraulic Conductivity Using Double-Ring Infiltrometers and Numerical Simulation. Soil Science Society of America Journal 71, 1667. https://doi.org/10.2136/sssaj2006.0227
Lamy, E., Lassabatere, L., Bechet, B., Andrieu, H., 2009. Modeling the influence of an artificial macropore in sandy columns on flow and solute transfer. Journal of Hydrology 376, 392–402. https://doi.org/10.1016/j.jhydrol.2009.07.048
Lassabatere, L., Angulo-Jaramillo, R., Soria Ugalde, J.M., Cuenca, R., Braud, I., Haverkamp, R., 2006. Beerkan estimation of soil transfer parameters through infiltration experiments—BEST. Soil Science Society of America Journal 70, 521. https://doi.org/10.2136/sssaj2005.0026
Lassabatere, L., Angulo-Jaramillo, R., Soria-Ugalde, J.M., Šimůnek, J., Haverkamp, R., 2009. Numerical evaluation of a set of analytical infiltration equations: EVALUATION INFILTRATION. Water Resources Research 45, n/a-n/a. https://doi.org/10.1029/2009WR007941
Lassabatere, L., Spadini, L., Delolme, C., Février, L., Galvez Cloutier, R., Winiarski, T., 2007. Concomitant Zn–Cd and Pb retention in a carbonated fluvio-glacial deposit under both static and dynamic conditions. Chemosphere 69, 1499–1508. https://doi.org/10.1016/j.chemosphere.2007.04.053
Lassabatere, L., Yilmaz, D., Peyrard, X., Peyneau, P.E., Lenoir, T., Šimůnek, J., Angulo-Jaramillo, R., 2014. New Analytical Model for Cumulative Infiltration into Dual-Permeability Soils. Vadose Zone Journal 0, 0. https://doi.org/10.2136/vzj2013.10.0181
Lauren, J.G., Wagnet, R., Bouma, J., Wosten, J., 1988. Variability of saturated hydraulic conductivity in a Glossaquic Hapludalf with macropores. Soil Science 145, 20–28.
Lee, D.M., Elrick, D.E., Reynolds, W.D., Clothier, B.E., 1985. A comparison of three field methods for measuring saturated hydraulic conductivity. Canadian journal of soil science 65, 563–573.
Lewis, T.E., Blasdell, B., Blume, L.J., 1990. Collection of Intact Cores from a Rocky Desert and a Glacial Till Soil. Soil Science Society of America Journal 54, 938–940. https://doi.org/10.2136/sssaj1990.03615995005400030057x
Mendoza, G., Steenhuis, T.S., 2002. Determination of hydraulic behavior of hillsides with a hillslope infiltrometer. Soil Science Society of America Journal 66, 1501–1504.
Merva, G.E., 1979. Falling head permeameter for field investigation of hydraulic conductivity. American Society of Agricultural Engineers.
Montgomery, D.R., Dietrich, W.E., 1995. Hydrologic Processes in a Low-Gradient Source Area. Water Resour. Res. 31, 1–10. https://doi.org/10.1029/94WR02270
Mubarak, I., Mailhol, J.C., Angulo-Jaramillo, R., Ruelle, P., Boivin, P., Khaledian, M., 2009. Temporal variability in soil hydraulic properties under drip irrigation. Geoderma 150, 158–165. https://doi.org/10.1016/j.geoderma.2009.01.022
Muller, R.N., Hamilton, M.E., 1992. A simple, effective method for determining the bulk density of stony soils. Communications in Soil Science and Plant Analysis 23, 313–319. https://doi.org/10.1080/00103629209368590
Niedda, M., Pirastru, M., 2013. Hydrological processes of a closed catchment-lake system in a semi-arid Mediterranean environment. Hydrol. Process. 27, 3617–3626. https://doi.org/10.1002/hyp.9478
Niedda, M., Pirastru, M., Castellini, M., Giadrossich, F., 2014. Simulating the hydrological response of a closed catchment-lake system to recent climate and land-use changes in semi-arid Mediterranean environment. Journal of Hydrology 517, 732–745. https://doi.org/10.1016/j.jhydrol.2014.06.008
Pachepsky, Y., Hill, R.L., 2017. Scale and scaling in soils. Geoderma, Structure and function of soil and soil cover in a changing world: characterization and scaling 287, 4–30. https://doi.org/10.1016/j.geoderma.2016.08.017
Pachepsky, Y.A., Guber, A.K., Yakirevich, A.M., McKee, L., Cady, R.E., Nicholson, T.J., 2014. Scaling and Pedotransfer in Numerical Simulations of Flow and Transport in Soils. Vadose Zone Journal 13. https://doi.org/10.2136/vzj2014.02.0020
Pirastru, M., Marrosu, R., Di Prima, S., Keesstra, S., Giadrossich, F., Niedda, M., 2017. Lateral Saturated Hydraulic Conductivity of Soil Horizons Evaluated in Large-Volume Soil Monoliths. Water 9, 862. https://doi.org/10.3390/w9110862
Pirastru, M., Niedda, M., Castellini, M., 2014. Effects of maquis clearing on the properties of the soil and on the near-surface hydrological processes in a semi-arid Mediterranean environment. Journal of Agricultural Engineering 45, 176. https://doi.org/10.4081/jae.2014.428
Prédélus, D., Lassabatere, L., Louis, C., Gehan, H., Brichart, T., Winiarski, T., Angulo-Jaramillo, R., 2017. Nanoparticle transport in water-unsaturated porous media: effects of solution ionic strength and flow rate. J Nanopart Res 19, 104. https://doi.org/10.1007/s11051-017-3755-4
Regan, M.P., 2000. Perched water table dynamics and hydrologic processes in an eastern Palouse catchment (M.S. thesis). University of Idaho, Moscow.
Reynolds, W., Elrick, D., Youngs, E., 2002. 3.4.3.2.a. Single-ring and double- or concentric-ring infiltrometers. Methods of Soil Analysis, Part 4, Physical Methods, J.H. Dane and G.C. Topp co-editors, Number 5 in the Soil Science Society of America Book Series, Soil Science Society of America, Inc. Madison, Wisconsin, USA, pp. 821-826.
Reynolds, W.D., 1993. Saturated hydraulic conductivity: Field measurement. M.R. Carter, editor, Soil sampling and methods of analysis. Canadian Society of Soil Science, Lewis Publishers, Boca Raton, FL. 599–613.
Reynolds, W.D., Elrick, D.E., 2005. Chapter 6 Measurement and characterization of soil hydraulic properties. In J. Álvarez-Benedí, & R. Muñoz-Carpena (Co-Eds.), Soil-water-solute process characterization – An integrated approach. Boca Raton: CRC Press.
Scanlon, B.R., Keese, K.E., Flint, A.L., Flint, L.E., Gaye, C.B., Edmunds, W.M., Simmers, I., 2006. Global synthesis of groundwater recharge in semiarid and arid regions. Hydrological Processes 20, 3335–3370. https://doi.org/10.1002/hyp.6335
Shirazi, M.A., Boersma, L., 1984. A unifying quantitative analysis of soil texture. Soil Science Society of America Journal 48, 142–147.
Soil Survey Staff, 2006. Keys to Soil Taxonomy, 10th ed. NRCS, Washington, DC.
Starr, J.L., Sadeghi, A.M., Pachepsky, Y.A., 2005. Monitoring and Modeling Lateral Transport through a Large In Situ Chamber. Soil Science Society of America Journal 69, 1871–1880. https://doi.org/10.2136/sssaj2004.0162
Sukhija, B.S., Reddy, D.V., Nagabhushanam, P., Hussain, S., 2003. Recharge processes: piston flow vs preferential flow in semi-arid aquifers of India. Hydrogeology Journal 11, 387–395. https://doi.org/10.1007/s10040-002-0243-3
Šimůnek, J., Jarvis, N.J., van Genuchten, M.T., Gärdenäs, A., 2003. Review and comparison of models for describing non-equilibrium and preferential flow and transport in the vadose zone. Journal of Hydrology 272, 14–35. https://doi.org/10.1016/S0022-1694(02)00252-4
Vepraskas, M.J., Williams, J.P., 1995. Hydraulic conductivity of saprolite as a function of sample dimensions and measurement technique. Soil Science Society of America Journal 59, 975–981.
Vörösmarty, C.J., Green, P., Salisbury, J., Lammers, R.B., 2000. Global Water Resources: Vulnerability from Climate Change and Population Growth. Science 289, 284–288. https://doi.org/10.1126/science.289.5477.284
Warrick, A.W., 1998. Spatial variability. In: Hillel, D. (Ed.), Environmental Soil Physics. Academic Press, San Diego, CA, pp. 655–675.
Yilmaz, D., Lassabatere, L., Angulo-Jaramillo, R., Deneele, D., Legret, M., 2010. Hydrodynamic Characterization of Basic Oxygen Furnace Slag through an Adapted BEST Method. Vadose Zone Journal 9, 107. https://doi.org/10.2136/vzj2009.0039
Young, S.K., 1998. Soil hydrology in an eastern Palouse micro-catchment underlain by a fragipan (M.S. thesis). University of Idaho, Moscow.
Zaslavsky, D., Rogowski, A.S., 1969. Hydrologic and Morphologic Implications of Anisotropy and Infiltration in Soil Profile

Di Prima, S., Marrosu, R., Lassabatere, L., Angulo-Jaramillo, R., Pirastru, M., 2018. In situ characterization of preferential flow by combining plot- and point-scale infiltration experiments on a hillslope. Journal of Hydrology 563, 633–642. https://doi.org/10.1016/j.jhydrol.2018.06.033

Development. Soil Science Society of America Journal 33, 594–599. https://doi.org/10.2136/sssaj1969.03615995003300040031x

Zimmermann, A., Schinn, D.S., Francke, T., Elsenbeer, H., Zimmermann, B., 2013. Uncovering patterns of near-surface saturated hydraulic conductivity in an overland flow-controlled landscape. Geoderma 195–196, 1–11. https://doi.org/10.1016/j.geoderma.2012.11.002

Zobeck, T.M., Fausey, N.R., Al-Hamdan, N.S., 1985. Effect of Sample Cross-Sectional Area on Saturated Hydraulic Conductivity in Tow Structured Clay Soils. Transactions of the ASAE 28, 791–794. https://doi.org/10.13031/2013.32339

Di Prima, S., Marrosu, R., Lassabatere, L., Angulo-Jaramillo, R., Pirastru, M., 2018. In situ characterization of preferential flow by combining plot- and point-scale infiltration experiments on a hillslope. Journal of Hydrology 563, 633–642. https://doi.org/10.1016/j.jhydrol.2018.06.033